J. Cent. South Univ. (2019) 26: 1747−1754
DOI: https://doi.org/10.1007/s11771-019-4130-7

Springer

Collapse mode of rock mass induced by a concealed karst cave above a deep cavity

HUANG Fu(黄阜), ZHANG Min(张敏), JIANG Zhen(蒋震)

School of Civil Engineering, Changsha University of Science and Technology, Changsha 410114, China

Abstract: Reliable prediction of the potential collapse region of rock mass is a key challenge for deep underground cavity excavation, especially if a concealed karst cave is located above the excavated cavity. Because of the effect of the blast vibration, a possible collapse would occur at a certain region between the concealed karst cave and the excavated cavity. This paper aims to study the roof collapse of a deep buried cavity induced by a concealed karst cave base on a two-dimensional failure mechanism by using upper bound theorem. The failure mechanism is constituted by arbitrary curves which is similar to the collapse observed in an actual cavity excavation. The shape and range of the collapse block is determined by virtual work equation in conjunction with variational approach. The results obtained by the presented approach are approximate with the numerical results provided by finite difference code, which indicates that the proposed method in this work is valid.

Key words: concealed karst cave; deep rectangular cavity; collapse mechanism; rock mass

Cite this article as: HUANG Fu, ZHANG Min, JIANG Zhen. Collapse mode of rock mass induced by a concealed karst cave above a deep cavity [J]. Journal of Central South University, 2019, 26(7): 1747−1754. DOI: https://doi.org/10.1007/s11771-019-4130-7.

1 Introduction

The stability of rock pillar is often a concern during tunnel construction and underground project excavation in a karst terrain. Presently, the geophysical prospecting technique is widely used to predict concealed karst caves and other geological defects in tunnel engineering. However, due to the limitation of the prediction techniques, the position and the size of a karst cavity cannot be detected precisely in the prospecting stage. Because it is difficult to determine the position of the karst cavity accurately, the planned underground engineering may be very close to a concealed karst cave and the blast vibration resulting from the excavation would make the rock pillar collapse. Especially if a karst cave is located above the underground engineering, a large number of fillers would swarm into the tunnel under the effect of huge pressure of the karst cave. As a result of the fillers of the karst cave, the tunnel would be buried in a remarkably short period of time. More seriously, the occurrence of a collapse of rock pillar is instantaneous with no warning time for the builders. Therefore, the collapse of rock pillar induced by an adjacent karst cave in tunnel construction may lead to serious economic losses and has drawn the attention of many investigators in this area.

To investigate the stability of the surface cover for a karst cavity, XIAO et al [1] designed a laboratory experiment and a physical model. By simulating the groundwater level changes in a karst cave, the authors obtained the influences of groundwater level fluctuation on the stability of surface cover above a karst cave. Employing a fluid-solid coupling model, ZHAO et al [2] investigated the mechanism of water inrush from a

Foundation item: Projects(51878074, 51678071) supported by the National Natural Science Foundation of China
Received date: 2019-01-23; **Accepted date:** 2019-04-26
Corresponding author: HUANG Fu, PhD, Associate Professor; Tel: +86-13975146439; E-mail: hfcsust@csust.edu.cn; ORCID: 0000-0002-5868-8659

karst cave in front of a tunnel face in conjunction with the strength reduction method. Based on the result of the numerical simulation, they proposed a formula to calculate a minimum thickness of a rock stratum to avoid water swarming into the tunnel. CUI et al [3] summed up the main reasons which cause engineering problems encountered during the construction of diaphragm wall in karst area, and proposed a corresponding treatment technique. Based on an actual engineering, JIANG et al [4] employed a minimum model test to investigate the safety thickness of the rock pillar between a tunnel and a water-logged stratum. Finding that karst caves cause a risk to tunnel excavation, LI et al [5] proposed a method to detect the position of a concealed karst cave on the basis of displacement monitoring. Moreover, the validation of this method has been verified by studying the displacement rules of the monitoring points on tunnel arch ring obtained from numerical simulation.

Existing literatures show that the collapse of a rock mass around a underground engineering induced by karst cavity is common in tunnel engineering. It was difficult to find an effective method to determine the collapsing range of rock mass until FRALDI et al [6] proposed a new method on the basis of the upper bound theorem. Using this method, the authors derived the analytical expression of the collapse surface for rock mass above a cavern. The advantage of this method is that the final result is obtained by optimal calculation which makes the analytical solution consistent with the collapse surface observed in an actual project. Later on, FRALDI et al [7, 8] employed this method to study the collapse of roof for a railway tunnel and roof collapse by progressive failure. This method not only provides a simple and useful way of analyzing the collapse range of surrounding rock mass for tunnel, but also avoids the shortcomings of construction of a complex upper failure mechanism. Consequently, some investigators continued to study the collapse mechanism of tunnel roof with this method. With a great deal of attention paid recently to this issue, many in-depth studies have been conducted with remarkable achievements.

Finding that the method proposed by FRALDI et al [6] is a valid way to investigate the collapse of a cavity roof, some investigators have used this method to study the collapse resulting from adjacent karst cavity in tunnel construction. HUANG et al [9] used this method to study the collapse from the bottom of a tunnel induced by a concealed karst cavity. Though the achievement provided a useful way of analyzing the collapse in tunnel construction induced by a karst cavity beneath a tunnel, the mechanism of roof collapse for a cavity resulting from a concealed karst cave is still unclear.

This paper focuses on the prediction of collapse region for a deep buried cavity roof which results from a concealed karst cave. On the basis of the feature of the roof collapse above a deep rectangular cavity, a failure mechanism is constructed by using arbitrary curves. Employing this failure mechanism, we obtained the analytical formula of the collapse surface in the framework of the bound theorems of classical plasticity in conjunction with a variational approach. The shape and range of collapse blocks are drawn on the basis of the theoretical calculation. The study may help geotechnical engineers to determine the size and location of a possible collapse caused by a concealed karst cave in deep buried cavity excavation.

2 Concealed karst cave inducing failure mechanism

A karst cave would induce the roof collapse in underground cavity excavation, especially if the concealed karst cave is located above the cavity. When the blast vibration transfers to the rock mass between the karst cave and the underground cavity, the rock mass may collapse under the effect of gravity and filler pressure. Thus, this study aims to study the collapse mechanism of the rock mass induced by the concealed karst cave above an underground cavity. To satisfy this purpose, a two-dimensional axis-symmetrical failure mechanism which reflects the roof collapse feature of the cavity is constructed. For reasons of mathematical convenience, it is assumed that the karst cave located above a rectangular cavity is circular. Moreover, the radius of the karst cave is R and the distance between the karst cave and the underground cavity is H. Two arbitrary curves extend from the cavity roof to the bottom of the karst cave. Because the failure mechanism is assumed to be axis-symmetrical, the two curves which are symmetric about y-axis constitute the collapse block.

An arbitrary curve indicates that the constructed failure mechanism is not restricted to the predefined line type. Consequently, the collapse block which is constituted by the arbitrary curves would be more consistent with the collapse mode observed in an actual project. Due to the effect of blast vibration, a slight slide would occur along the boundary of the collapse block. So, the boundary which is composed of the two curves $f(x)$ can also be known as velocity discontinuity curves. To study the roof collapse mechanism of the cavity induced by the concealed karst cave, it is necessary to derive the formula of the velocity discontinuity curve. Using the formula of the velocity discontinuity curve, the potential collapse range is obtained.

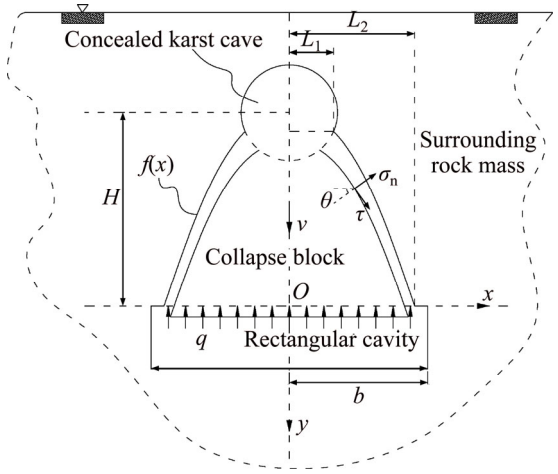

Figure 1 Failure mechanism of rock mass above deep rectangular cavity induced by karst cave

3 Calculation process of upper bound solution for collapse surface

Since the collapse block is detached from the cavity roof, the plastic flow occurs along the boundary of the collapse block. Based on the relationship between plastic stress and plastic strain rate, the rate of the energy dissipation for a random point in the plastic flow region is derived from the plastic stress/strain rate relation. As pointed out by CHEN [10], the stress/strain rate relation can be deduced from the normality condition related to a yield function. Hoek-Brown nonlinear failure criterion, which can be employed to evaluate the strength of rock mass from tightly interlocked to very poor quality, is widely applied in tunnel stability analysis [11−18]. This study also employs the H-B failure criterion to describe the failure characteristic of the rock mass caused by a concealed karst cave in a deep buried cavity excavation. Assuming the velocity discontinuity field satisfies the H-B yield condition, the plastic potential is obtained

$$\Omega = \tau - A\sigma_{ci}\left(\frac{\sigma_n - \sigma_{tm}}{\sigma_{ci}}\right)^B \tag{1}$$

where τ and σ_n are normal and shear stress, respectively; A and B are material constants; σ_{ci} is the uniaxial compressive strength. Moreover, σ_{tm} is the tensile strength of the rock mass.

Based on the relationship between plastic potential and plastic strain rate, the rate of energy dissipation for a random point on the collapse boundary is given by:

$$\begin{aligned} D &= \sigma_n\dot{\varepsilon}_n + \tau\dot{\gamma}_n \\ &= \{\sigma_{tm} - \sigma_{ci}[ABf'(x)]^{\frac{1}{1-B}}(1-B^{-1})\}\frac{1}{\sqrt{1+f'(x)^2}}\frac{v}{t} \end{aligned} \tag{2}$$

where $\dot{\varepsilon}_n$ and $\dot{\gamma}_n$ are normal and shear plastic strain rate, respectively; $f(x)$ is the analytical expression of the velocity discontinuity curve; v is the velocity vector of the collapse block; $f'(x)$ is the first derivative of $f(x)$; and t is the thickness of the velocity discontinuity curve. The whole rate of energy dissipation in this failure mechanism can be computed by an integral.

$$\begin{aligned} P_D &= \int_{L_1}^{L_2} D\sqrt{1+f'(x)^2}\,\mathrm{d}x \\ &= \int_{L_1}^{L_2}\left\{\sigma_{tm} - \sigma_{ci}[ABf'(x)]^{\frac{1}{1-B}}(1-B^{-1})\right\}\frac{v}{t}\mathrm{d}x \end{aligned} \tag{3}$$

where L_1 and L_2 are the half length of the top and bottom of the collapse surface respectively. Furthermore, the external rate of work is generated by external loads which are composed of the weight of surrounding rock, filler pressure of karst cave and supporting pressure. The rate of work produced by self weight of the collapse block is

$$P_\gamma = \gamma[\int_0^{L_1} g(x)\mathrm{d}x + \int_{L_1}^{L_2} f(x)\mathrm{d}x]v \tag{4}$$

where γ is the unit weight of the rock mass, and $g(x)$ is the formula of the karst cave. Because the karst cave is a circle, the equation of the $g(x)$ is given by

$$g(x) = \sqrt{b^2 - x^2} - H \tag{5}$$

The work rate of the filler pressure is written as

$$P_T = TL_1 \frac{v}{b} \tag{6}$$

in which T is pressure of fillers in a karst cave and b is the half length of the underground cavity. Moreover, the work rate of the supporting pressure for the underground cavity is written in the form:

$$P_q = -L_2 q v \tag{7}$$

in which q is the supporting pressure. According to CHEN [10], the upper bound solution of the equation for the collapse region is deduced from the virtual work equation which is constituted by the total internal energy dissipation rate and the external work rate. Thus, an objective function ξ which is expressed by the difference of the total internal energy dissipation rate and the external work rate is established:

$$\begin{aligned}\xi &= P_D - P_\gamma - P_T - P_q \\ &= v\int_{L_1}^{L_2} \{\sigma_{\mathrm{tm}} - \sigma_{\mathrm{ci}}[ABf'(x)]^{\frac{1}{1-B}}(1-B^{-1}) - \gamma f(x)\}\mathrm{d}x - \\ &\quad \gamma v\int_0^{L_1} g(x)\mathrm{d}x - TL_1\frac{v}{b} + L_2 q v \\ &= v\int_{L_1}^{L_2} \psi[f(x), f'(x), x]\mathrm{d}x - \gamma v\int_0^{L_1} g(x)\mathrm{d}x - \\ &\quad TL_1\frac{v}{b} + L_2 q v\end{aligned} \tag{8}$$

where ψ is a functional which is defined as:

$$\psi[f(x), f'(x), x] = \sigma_{\mathrm{tm}} - \sigma_{\mathrm{ci}}[ABf'(x)]^{\frac{1}{1-B}}(1-B^{-1}) - \gamma f(x) \tag{9}$$

Furthermore, based on the upper bound rules, the solution derived from the virtual work equation is one of the upper bound solutions. It means that the real upper bound solution of $f(x)$ is the one which leads the ξ to reaching an extremum. However, objective function ξ is determined by ψ. Consequently, when the functional ψ reaches an extremum, the corresponding $f(x)$ is the real solution of $f(x)$. The variational principle indicates that the functional ψ has an extremum when $f(x)$ satisfies the condition:

$$\frac{\partial \psi}{\partial f(x)} - \frac{\mathrm{d}}{\mathrm{d}x}\left[\frac{\partial \psi}{\partial f'(x)}\right] = 0 \tag{10}$$

By substituting Eq. (9) into Eq. (10), a differential equation is derived

$$-\gamma + \frac{\sigma_{\mathrm{ci}}}{1-B}(AB)^{\frac{1}{1-B}}[f'(x)]^{\frac{2B-1}{1-B}} f''(x) = 0 \tag{11}$$

After integral operation, the analytical expression of $f(x)$ can be derived as

$$f(x) = A^{-\frac{1}{B}}\left(\frac{\gamma}{\sigma_{\mathrm{ci}}}\right)^{\frac{1-B}{B}}\left(x - \frac{c_0}{\gamma}\right)^{\frac{1}{B}} - c_1 \tag{12}$$

where c_0 and c_1 are two integration constants. Substituting Eq. (12) into Eq. (8), the expression of ξ is:

$$\begin{aligned}\xi = -\frac{1}{1+B}A^{-\frac{1}{B}}\sigma_{\mathrm{ci}}^{\frac{B-1}{B}}\gamma^{\frac{1}{B}}\Bigg[\left(L_2 - \frac{c_0}{\gamma}\right)^{\frac{1+B}{B}} - \\ \left(L_1 - \frac{c_0}{\gamma}\right)^{\frac{1+B}{B}}\Bigg] + (c_1\gamma + \sigma_{\mathrm{tm}})(L_2 - L_1) - \gamma H L_1 + \\ \frac{1}{2}L_1\gamma\sqrt{b^2 - L_1^2} + b^2\gamma\arcsin\left(\frac{L_1}{b}\right) - \frac{TL_1}{b} + L_2 q\end{aligned} \tag{13}$$

To derive the final expression of $f(x)$, the values of c_0 and c_1 should be determined. So, it is necessary to obtain several boundary conditions which can be used to calculate the unknown parameters. Based on the distribution characteristics of shear stress, there is no such stress at the point of the collapse surface and the karst cave. Using this stress boundary condition, the value of c_0 is obtained.

$$c_0 = \gamma L_1 \tag{14}$$

Substituting Eq. (14) into Eq. (12), the analytical expression of $f(x)$ which includes L_1 and c_1 can be written in the form:

$$f(x) = A^{-\frac{1}{B}}\left(\frac{\gamma}{\sigma_{\mathrm{ci}}}\right)^{\frac{1-B}{B}}(x - L_1)^{\frac{1}{B}} - c_1 \tag{15}$$

Moreover, the velocity discontinuity curve $f(x)$ fits the geometric boundary conditions illustrated as follows:

$$\begin{cases} f(x = L_2) = 0 \\ f(x = L_1) = g(x = L_1) \end{cases} \tag{16}$$

By substituting Eqs. (5) and (15) into Eq.(16), nonlinear equations are obtained

$$\begin{cases} A^{-\frac{1}{B}}\left(\frac{\gamma}{\sigma_{\mathrm{ci}}}\right)^{\frac{1-B}{B}}(L_2 - L_1)^{\frac{1}{B}} = c_1 \\ c_1 = H - \sqrt{b^2 - L_1^2} \end{cases} \tag{17}$$

Obviously, there are three unknown constants in Eq. (17), and we have to find another equation to determine these unknown constants. Substituting Eq. (14) into Eq. (13), and equating the internal

dissipation of energy to the external rate of work, a new nonlinear equation is derived.

$$-\frac{1}{1+B}A^{-\frac{1}{B}}\sigma_{ci}^{\frac{B-1}{B}}\gamma^{\frac{1}{B}}(L_2-L_1)^{\frac{1+B}{B}}+(c_1\gamma+\sigma_{tm})(L_2-L_1)-\gamma HL_1+\frac{1}{2}L_1\gamma\sqrt{b^2-L_1^2}+b^2\gamma\arcsin\left(\frac{L_1}{b}\right)-\frac{TL_1}{b}+L_2q=0 \quad (18)$$

Using Eqs. (17) and (18), the values of L_1, L_1 and c_1 can be computed by a numerical method. Finally, substituting the values of L_1, L_1 and c_1 into Eq. (15), the final expression of $f(x)$ is expressed as follows:

$$f(x)=A^{-\frac{1}{B}}\left(\frac{\gamma}{\sigma_{ci}}\right)^{\frac{1-B}{B}}(x-L_1)^{\frac{1}{B}}+\sqrt{b^2-L_1^2}-H \quad (19)$$

4 Parameter analysis

During the excavation of a deep underground cavity, the impending roof collapse of the cavity would lead to economic losses or even human casualties. If a karst cave is located above the cavity, the possibility of the roof collapse for the cavity is greater. Thus, we have only to determine the collapse region induced by the concealed karst cave, and the corresponding treatment scheme can be proposed to prevent the roof collapse of the cavity. In this section, the range of the potential collapse region is plotted based on the analytical equation illustrated in Eq. (19), and the effect of relevant parameters on the range of the potential collapse region is discussed. As illustrated in Figures 2−7, the shapes of the collapse block for the parameters related to B=0.6−0.9, A=0.35−0.65, γ=18−24 kN/m^3, $\sigma_{tm}=\sigma_{ci}/100-\sigma_{ci}/60$, σ_{ci}=10 MPa, T=600−900 kPa, q=100−400 kPa, H=5 m, b=3 m are plotted. To investigate the change rule of collapse region changing with these parameters, a univariate analysis method is employed here. It can be found from Figures 2−7 that the greater values of A, B, and σ_{tm} tend to induce a larger range of the collapse block. In contrast, a higher value of γ leads to a decrease of the range for the collapse block. The change rules of these parameters are consistent with the conclusions presented in existing document [6], which indicate that the presented method is valid. Moreover, with the increase of T, the collapse region tends to increases. Inversely, the collapse

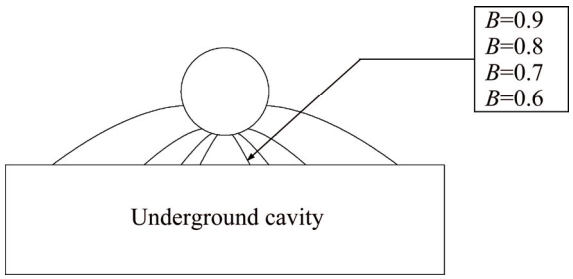

Figure 2 Effect of parameter B on shape and range for collapse block

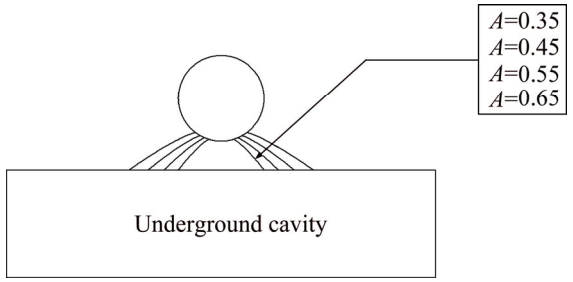

Figure 3 Effect of parameter A on shape and range for collapse block

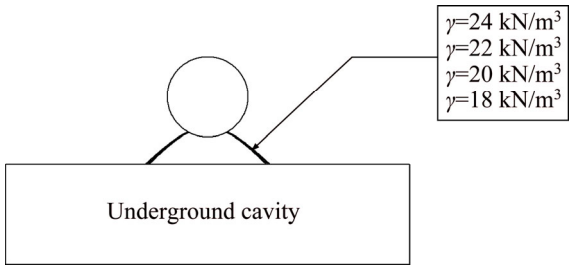

Figure 4 Effect of parameter γ on shape and range for collapse block

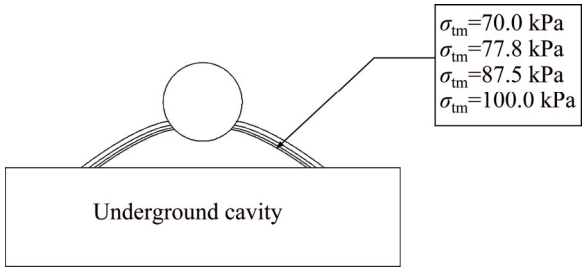

Figure 5 Effect of parameter σ_{tm} on shape and range for collapse block

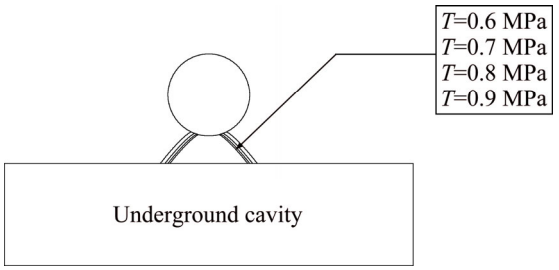

Figure 6 Effect of parameter T on shape and range for collapse block

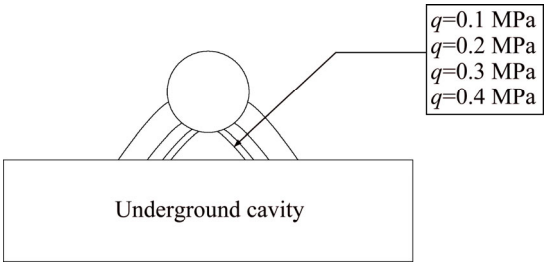

Figure 7 Effect of parameter q on shape and range for collapse block

region decreases with the increase of values of q. This implies that the karst caves with larger filler pressure would lead to a greater collapse region which is more difficult to treat for the underground cavity excavated in a karst terrain. However, strengthening the lining structure to increase supporting pressure is an effective way to control the development of the potential collapse region.

5 Comparison with numerical simulation results

Because this paper proposed a new method to calculate the collapse region of a rectangular cavity roof induced by a karst cave, it is necessary to verify the validity of the presented method. Numerical simulation technique is an effective way to conduct comparisons with theoretical results and numerous scholars have used this technique to achieve these comparisons [19−21]. In this work, the finite-difference code FLAC^{3D} is employed to simulate the roof collapse of rock mass for a rectangular cavity which induced by a karst cave. A numerical model with approximately 16432 zones and 21320 nodes is constructed which can be seen in Figure 8. The dimensions of this model are taken to be 90, 110 and 4 m in the transversal, vertical, and longitudinal directions. Furthermore, the diameter of the karst cave is 6 m and the width of the rectangular cavity is 30 m. Because the roof collapse occurs in the region between the karst cave and the excavated cavity, the mesh in this region is densified to increase the precision of the simulation.

The H-B yield criterion invoked in the FLAC is expressed by the major and minor principal stresses, whereas the H-B yield criterion employed in theoretical calculation is expressed by normal and shear stresses. Thus, several parameters in the two types of the H-B yield criterion are inconsistent.

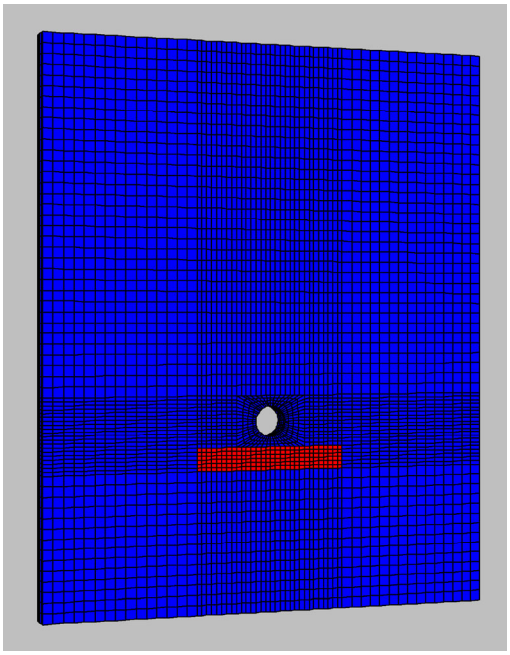

Figure 8 Numerical model of karst cavern existing above rectangular cavity

To compare the upper bound solution and the numerical result under the same condition, the parameters in one type of the H-B yield criterion should be converted into the other type equivalently. The method proposed by HOEK and BROWN [22] is employed here to achieve the equivalent conversion and a set of equivalent parameters for the two types of the mentioned criterion are illustrated in Table 1. Table 2 shows the relevant parameters used in numerical simulation.

Using the parameters illustrated in Table 2, the collapse of the cavity roof is simulated by using the

Table 1 Equivalent parameters for two types of H-B failure criterion

Parameter	Value
A	0.67
B	0.7
σ_{ci}/MPa	4
σ_{tm}/MPa	0.04
a	0.5
m_b	3.2855
S	0.0334
σ_{ci}/MPa	4
GSI	69

Notes: a, m_b, S and GSI are parameters in H-B failure criterion denoted by the major and minor principal stresses.

Table 2 Parameters used in numerical

γ/ (kN·m^{-3})	E/GPa	μ	σ_{ci}/MPa	a	m_b	S
25.0	2.3	0.32	4	0.5	3.2855	0.0334

Notes: E is elasticity modulus; μ is Poisson ratio.

model described in Figure 8. It is assumed in the excavation of the cavity that the rock mass at the excavation region is excavated instantaneously. Due to the excavation disturbance, a tensile (or shear) zone in the rock mass above the cavity crown may form. When the tensile (or shear) zones connect each other in this region, tensile (or shear) failure belt forms and the roof collapse above the cavity crown occurs. To investigate the roof collapse, the contours of shear strain increment for the model that reflect the shape and the region of the collapse block are obtained. It is found from Figure 9 that a shear failure belt which is colored green forms in the rock mass above the cavity roof and extends to the edge of the karst cavern. The shear failure belt is symmetric about the y-axis. To find the difference of the collapse surface derived from the theoretical calculation and the failure belt obtained from numerical simulation conveniently, the collapse surface provided from Eq. (19) is superimposed on Figure 9 with the equivalent parameters illustrated in Table 1. The shape of the collapse block provided by upper bound calculation is similar to the shear-failure belt obtained by the numerical simulation. Although the range of the shear-failure belt is larger than the analytical solution of the collapse region, the difference between the results provided by the two methods is acceptable. The result of the comparison between the two methods implies that the method presented in this paper is effective.

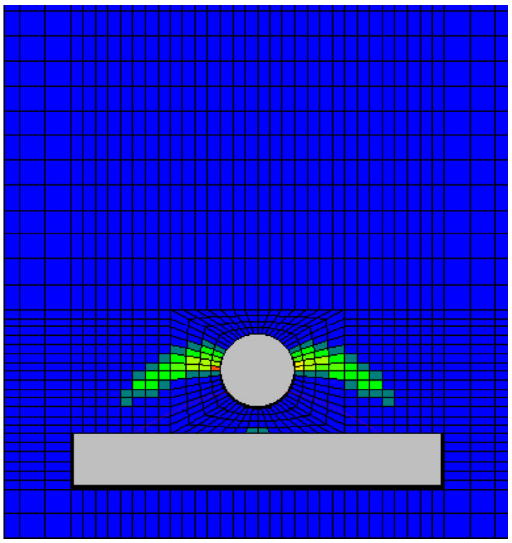

Figure 9 Comparison of collapse region derived from theoretical calculation and numerical simulation

6 Conclusions

For an underground cavity excavation in a karst terrain, the stability of rock mass above the excavated cavity crown is a key factor that is concerned most by engineers. This paper aims to investigate the roof collapse of a rectangular cavity induced by a concealed karst cave. A failure mechanism constituted by arbitrary curves is established, and upper bound solutions of collapse block above a rectangular cavity crown are derived from the upper bound theorem in conjunction with variational principle.

The upper bound solutions of a collapse block are compared with the results provided by numerical simulation technique. The solutions provide by the presented method agree with the numerical solutions, which indicates that the presented method is an effective method to predict the potential collapse region of rock mass.

Furthermore, parameter analysis shows that increasing γ and q led to a reduction in the range of collapse block, whereas the greater values of A, B, σ_{tm} and T tended to induce a larger collapse region. The change rules of the collapse region varying with these parameters imply that the karst cave with large filler pressure would cause a larger scale collapse of rock mass whereas strengthening the lining structure is an effective way to prevent the occurrence of the rock mass collapse for deep cavity.

References

[1] XIAO X X, XU M, DING Q Z, KANG X B, XIA Q, DU F. Experimental study investigating deformation behavior in land overlying a karst cave caused by groundwater level changes [J]. Environmental Earth Sciences, 2018, 77(3): 64−75.

[2] ZHAO Y L, PENG Q Y, WAN W, WANG W J, CHEN B. Fluid-solid coupling analysis of rock pillar stability for concealed karst cave ahead of a roadway based on catastrophic theory [J]. International Journal of Mining Science and Technology, 2014, 24: 737−745.

[3] CUI Q L, SHEN S L, XU Y S, WU H N, YIN Z Y. Mitigation of geohazards during deep excavations in karst regions with caverns: A case study [J]. Engineering Geology, 2015, 195: 16−27.

[4] JIANG H M, LI L, RONG X L, WANG M Y, XIA Y P, ZHANG Z C. Model test to investigate waterproof-resistant slab minimum safety thickness for water inrush geohazards [J]. Tunnelling and Underground Space Technology, 2017, 62: 35−42.

[5] LI S C, WU J, XU Z H, ZHOU L, ZHANG B. A possible prediction method to determine the top concealed karst cave based on displacement monitoring during tunnel construction [J]. Bulletin of Engineering Geology and the Environment, 2017. DOI: 10.1007/s10064-017-1060-1.

[6] FRALDI M, GUARRACINO F. Limit analysis of collapse mechanisms in cavities and tunnels according to the Hoek–Brown failure criterion [J]. International Journal of Rock Mechanics and Mining Sciences, 2009, 46: 665−673.

[7] FRALDI M, GUARRACINO F. Analytical solutions for collapse mechanisms in tunnels with arbitrary cross sections [J]. International Journal of Solids and Structures, 2010, 47: 216−223.

[8] FRALDI M, GUARRACINO F. Limit analysis of progressive tunnel failure of tunnels in Hoek-Brown rock masses [J]. International Journal of Rock Mechanics and Mining Sciences, 2012, 50: 170−173.

[9] HUANG F, ZHAO L H, LING T H, YANG X L. Rock mass collapse mechanism of concealed karst cave beneath deep tunnel [J]. International Journal of Rock Mechanics and Mining Sciences, 2017, 91: 133−138.

[10] CHEN W F. Limit analysis and soil plasticity [M]. Amsterdam: Elsevier, 1975.

[11] HUANG F, OU R C, LI Z L, YANG X L, LING T H. Limit analysis for the face stability of a shallow-shield tunnel based on a variational approach to the blow-out failure mode [J]. International Journal of Geomechanics, 2018, 18(6): 04018038.

[12] PAN Q, DIAS D. Three dimensional face stability of a rock tunnel subjected to seepage forces [J]. Tunnelling and Underground Space Technology, 2018, 71: 555−566.

[13] UKRITCHON B, KEAWSAWASVONG S. Stability of unlined square tunnels in Hoek-Brown rock masses based on lower bound analysis [J]. Computers and Geotechnics, 2019, 105: 249−264.

[14] ZHANG D B, LIU Z Z, ZHANG J H. A new failure mechanism for deep cavity and upper bound solution of supporting pressure [J]. Journal of Central South University, 2017, 24(9): 2082−2091.

[15] YANG X L, ZHANG S. Risk assessment model of tunnel water inrush based on improved attribute mathematical theory [J]. Journal of Central South University, 2018, 25(2): 379−391.

[16] XU J S, YANG X L. Seismic stability of 3D soil slope reinforced by geosynthetic with nonlinear failure criterion [J]. Soil Dynamics and Earthquake Engineering, 2019, 118: 86−97.

[17] LI Y X, YANG X L. Soil-slope stability considering effect of soil-strength nonlinearity [J]. International Journal of Geomechanics, 2019, 19(3): 04018201

[18] LI Z W, YANG X L. Kinematical analysis of active earth pressure considering tension crack, pore-water pressure and soil nonlinearity [J]. KSCE Journal of Civil Engineering, 2019, 23(1): 56−62.

[19] MOLLON G, DIAS D, SOUBRA A H. Continuous velocity fields for collapse and blowout of a pressurized tunnel face in purely cohesive soil [J]. International Journal for Numerical and Analytical Methods in Geomechanics, 2013, 37(13): 2061−2083.

[20] IBRAHIM E, SOUBRA A H, MOLLON G, RAPHAEL W, DIAS D, REDA A. Three-dimensional face stability analysis of pressurized tunnels driven in a multilayered purely frictional medium [J]. Tunnelling and Underground Space Technology, 2015, 49: 18−34.

[21] MOLLON G, PHOON K K, DIAS D, SOUBRA A H. Validation of a new 2D failure mechanism for the stability analysis of a pressurized tunnel face in a spatially varying sand [J]. Journal of Engineering Mechanics, 2011, 137(1): 8−21.

[22] HOEK E, BROWN E T. Practical estimate the rock mass strength [J]. International Journal of Rock Mechanics and Mining Sciences. 1997, 34: 1165−1186.

(Edited by HE Yun-bin)

中文导读

顶部存在隐伏溶洞的深埋地下硐室围岩塌落机理研究

摘要：可靠地预测由于地下工程施工导致的围岩塌落范围是地下工程施工中遇到的一个关键问题。尤其当地下硐室上方存在隐伏溶洞时，由于施工过程中爆破振动的影响，增大了地下硐室与隐伏溶洞之间围岩发生垮塌的可能性。针对这一现象，利用任意线型的曲线构建了由于隐伏溶洞诱发深埋硐室顶部围岩塌落破坏的二维破坏机制。在此基础上，基于极限分析上限定理的虚功率方程和变分法计算得到了深埋硐室顶部围岩塌落面的解析方程，并绘制了不同参数作用下深埋硐室顶部围岩塌落面的形状和范围。为了验证理论结果的正确性，将计算得到的围岩塌落面理论解和数值模拟得到的数值解进行了对比。分析表明：理论解和数值解基本一致，证明本文的理论计算结果是有效的。

关键词：隐伏溶洞；深埋矩形硐室；塌落机理；围岩